An Iteration-Free MoM Approach Based on Excitation Independent Characteristic Basis Functions for Solving Large Multiscale Electromagnetic Scattering Problems

Eugenio Lucente, Agostino Monorchio, *Senior Member, IEEE*, and Raj Mittra, *Life Fellow, IEEE*

***Abstract*—We describe a numerically efficient strategy for solving a linear system of equations arising in the Method of Moments for solving electromagnetic scattering problems. This novel approach, termed as the characteristic basis function method (CBFM), is based on utilizing characteristic basis functions (CBFs)—special functions defined on macro domains (blocks)—that include a relatively large number of conventional sub-domains discretized by using triangular or rectangular patches. Use of these basis functions leads to a significant reduction in the number of unknowns, and results in a substantial size reduction of the MoM matrix; this, in turn, enables us to handle the reduced matrix by using a direct solver, without the need to iterate. In addition, the paper shows that the CBFs can be generated by using a sparse representation of the impedance matrix—resulting in lower computational cost—and that, in contrast to the iterative techniques, multiple excitations can be handled with only a small overhead. Another important attribute of the CBFM is that it is readily parallelized. Numerical results that demonstrate the accuracy and time efficiency of the CBFM for several representative scattering problems are included in the paper.**

***Index Terms*—Characteristic basis functions (CBFs), electrically large, electromagnetic scattering, method of moments (MoM), radar cross section (RCS).**

I. Introduction

MOST OF THE existing frequency-domain method of moments (MoM) for analyzing arbitrary three-dimensional (3-D) electromagnetic structures utilize sub-domain basis functions, typically Rao, Wilton, and Glisson types [1] whose dimensions are on the order of $\lambda/10$. This in turn, poses a considerable burden on the CPU, both in terms of memory and solve-time when dealing with electrically large problems in terms of the wavelength. Hybridization of the MoM with asymptotic techniques, such as physical optics (PO) or ray-based geometrical theory of diffraction (GTD) methods, has been proposed by a number of authors [2]–[4] to circumvent these limitations. However, this type of approach has only seen limited applications, e.g., the modeling of a small antenna mounted on a large platform, because of the difficulties in finding a systematic way to merge the two methods. Recently, a number of techniques have been proposed to circumvent the problems of excessive memory and solve-time associated with large MoM matrices. The impedance matrix localization (IML) technique [5] replaces the MoM matrix by one with localized clumps of large elements. The use of wavelet basis functions [6] reduces the solution time by a constant factor but not the computational complexity. The complex multipole beam approach (CMBA) [7] represents the scattered field in a series of beams produced by multipole sources located in the complex space, but it is efficient only for smooth surfaces. The multilevel matrix decomposition algorithm (MLMDA) [8] carries out a fast matrix-vector multiplication by decomposing the MoM matrix into a large number of blocks, each describing the interaction between distant scatterers. The fast mulitpole method (FMM) [9] and its extension, the multilevel fast multipole algorithm (MLFMA) [10], realize a saving in the memory requirements by storing only the near-field interaction part of the large matrix. They also improve the time performance by accelerating the matrix-vector multiplications needed in the iterative solvers in a highly efficient manner using a spherical harmonic expansion technique. However, most of the techniques mentioned above still rely upon iteration methods to solve large problems, and this can lead to convergence difficulties when dealing with objects with multi-scale features. Recently, it has been shown that the use of high-level basis functions, defined over electrically large geometrical domains, can significantly reduce the number of unknowns. For instance, the macro basis function (MBF) and the sub-domain multilevel approach (SMA) [11] have been recently proposed to handle large planar antenna arrays. The above approaches are suitable for planar microstrip circuits and antennas, however their application to more general objects normally encountered in the EM scattering problems is not obvious, and, they do not directly account for the mutual coupling effect between different portions of the geometry.

More recently, the characteristic basis functions method (CBFM) [12] has been proposed to solve large problems. It uses a set of high-level basis functions, called CBFs that are specially constructed to fit the problem geometry by incorporating the physics of the problem into their generation. The

Manuscript received July 13, 2006; revised November 8, 2007.

E. Lucente and A. Monorchio are with the Department of Information Engineering, University of Pisa, I-56122 Pisa, Italy and also with the Electromagnetic Communication Laboratory, Pennsylvania State University, University Park, PA 16802 USA (e-mail: eugenio.lucente@iet.unipi.it; a.monorchio@iet.unipi.it).

R. Mittra is with the Electromagnetic Communication Laboratories, Pennsylvania State University, University Park, PA 16802 USA (e-mail: mittra@engr.psu.edu).

Color versions of one or more of the figures in this paper are available online at http://ieeexplore.ieee.org.

Digital Object Identifier 10.1109/TAP.2008.919166

CBFM differs from the other entire-domain approaches in several aspects. First, the technique is more general, and can be applied to an arbitrary geometry; second, it includes the mutual coupling effects rigorously and systematically; third, it leads to small-size matrices, called reduced-matrices, that are sparse and well-conditioned in nature; fourth, and perhaps the most important attribute of the CBFM, is that it only utilizes direct solvers rather than iterative methods; hence it does not suffer from convergence problems and can solve multiple excitation problems efficiently. The CBFM also realizes a sizable reduction in the storage requirement, enabling it to handle very large problems that cannot be dealt with by using conventional techniques. In this paper, we propose further improvements of the original version of CBFM that bypass the computation of the secondary basis functions; allow us to generate the CBFs by using a sparse representation of impedance matrix; and handle multiple excitations with only a small overhead. In addition, the CBFM is highly parallelizable, which is an important and desirable attribute, since a computer cluster is almost always used to solve a large problem.

The paper is organized as follows: we begin by describing the general theoretical formulation in Section II, with particular emphasis on geometrical block partitioning and multiple Plane Wave excitations. This is followed, in Section III, by a description of the sparse MoM impedance matrix approach to generating the macro-domain basis functions. Finally, in Section IV, we present some results that validate the efficiency and accuracy of the formulation.

II. Formulation

The application of the conventional MoM formulation, based on a subsectional basis functions, to the electric field integral equation (EFIE) leads to a dense, complex linear system of the form

$$\mathbf{Z} \cdot \mathbf{J} = \mathbf{V} \tag{1}$$

where $\mathbf{Z}$ is the generalized impedance matrix of dimension $N \times N$, $\mathbf{J}$ and $\mathbf{V}$ are $N \times 1$ vectors, and N is the number of unknowns. For large and complex problems, the matrix system (1) is used to solve for typically thousands of unknowns, and this poses a burden on computer memory and CPU time, since they increase as $O(N^2)$ and $O(N^3)$, respectively. Moreover, the size of the MoM impedance matrix becomes prohibitive for direct solvers when N is large, prompting one to use iterative solvers. However, the latter suffer from convergence difficulties when (1) is ill-conditioned, and, furthermore, they require solving the system anew for each excitation. The use of macro-domain basis function has the advantages that it leads to a reduced matrix that can be solved directly because it is much smaller than that of the original MoM, without requiring preconditioners. Moreover, multiple right hand sides are handled efficiently once the LU decomposition of the reduced matrix has been carried out.

The modified CBFM begins with dividing the geometry of the object to be analyzed into blocks, for instance M, characterizing these parts alone by using the so called primary characteristic basis functions, which not only represent the localized solution but also account for the interactions between the self-blocks and the remaining blocks. There is no limitation on the number and size of blocks. The upper size is bounded by the available RAM needed to handle the self-blocks that are solved to generate the CBFs. Typically, the block size ranges from a few hundred to a few thousand sub-domain type of unknowns.

Next a set of N^{PWS} primary CBFs are constructed for each block by exciting it with Plane Waves (PWs) incident from N^{PWS} angles (see Fig. 1). The number of PWs angles is deliberately overestimated, initially, so that the CBFs would be invariant with respect to the size of the block, the shape of the geometry under investigation, and can account for evanescent waves, if desired. Subsequently, the redundant information due to the overestimation is eliminated via the use of a singular value decomposition (SVD). Moreover, it is important to observe that, for a scatterer compactly supported within a sphere of radius a there is a sharp cutoff after which the asymptotic behavior of the singular values takes hold. Fig. 2 shows the distribution of the normalized singular values for the corner reflector case, which is presented in the numerical section as the last example. Distributions of the singular values, plotted for different blocks, show a sharp transition region where the cutoff occurs. This cut off can be estimated analytically using techniques analogous to the ones presented in [13]. Furthermore, a general discussion should also consider the relationship between spatial bandwidth of the scattered fields and degrees of freedom [14], which is not instrumental to our procedure and is beyond the scope of this paper. To this end, we overestimated this parameter that represents a lower bound to ensure the necessary accuracy. The advantages of following this procedure is that it enables us to solve for multiple excitations using the same reduced matrix with a significant time-saving since only the right hand side $(r.h.s.)$ of the reduced system needs to be computed for a new excitation. As a result, this approach is computationally more efficient than the original version of the CBFM [12].

For the sake of illustration, we consider a thin plate which is divided into 25 blocks, shown in Fig. 3. Although, in general, the blocks can have different sizes, we assume that they have approximately the same dimension N_b in terms of number of unknowns.

In order to compute the primary CBFs, all blocks are extended by a fixed amount Δ (typically 0.2λ to 0.4λ) in all directions, with the exception of free edges, to avoid a singular behavior in the current distribution within the original block introduced by the truncation that creates fictitious edges. Each of the M extended blocks are represented by the $N_{be} \times N_{be}$ self-impedance matrix $\mathbf{Z_{ii}}$, where $i = 1, 2, \ldots, M$, and N_{be} is the number of unknowns in the extended blocks. The matrix $\mathbf{Z_{ii}}$ is extracted from the original MoM matrix by using a matrix segmentation procedure. The concept of MoM matrix segmentation is illustrated in Fig. 4, where the extended and individual blocks are shown in dotted line and solid line, respectively. The self-impedance matrix is then used to generate the primary CBFs induced on a given block by exciting the block with a set of windowed plane waves, impinging upon the object with different incident angles (θ, φ), and with two linear different polarizations.

Let N_θ and N_ϕ indicate the number of samples in elevation and azimuth (θ and ϕ, respectively). This results in a total of $N^{\mathrm{PWS}} = N_\phi N_\theta$ plane wave excitations, which are arranged in

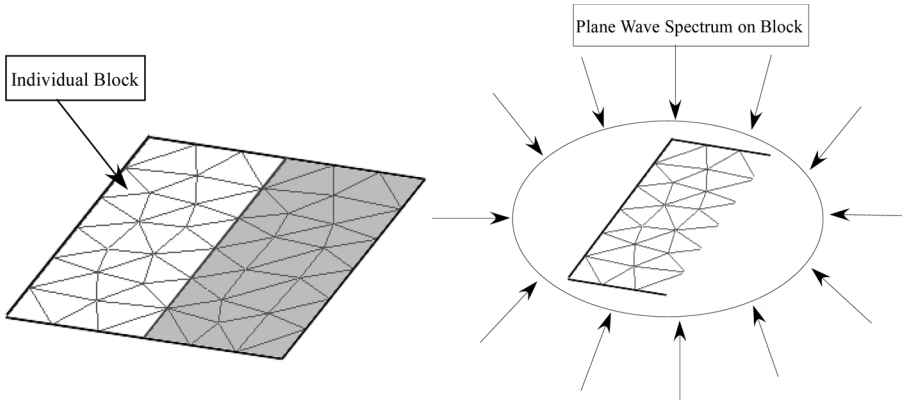

Fig. 1. Plane wave spectrum on a single block.

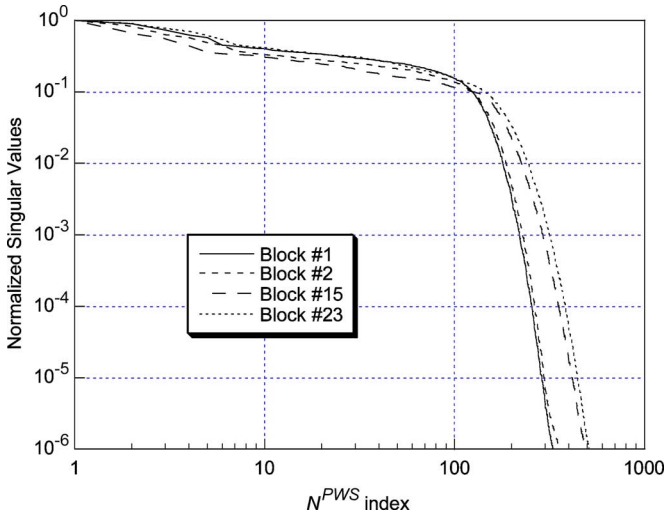

Fig. 2. Distributions of the normalized singular values for some blocks of example *iv*, as a function of the total plane wave samples.

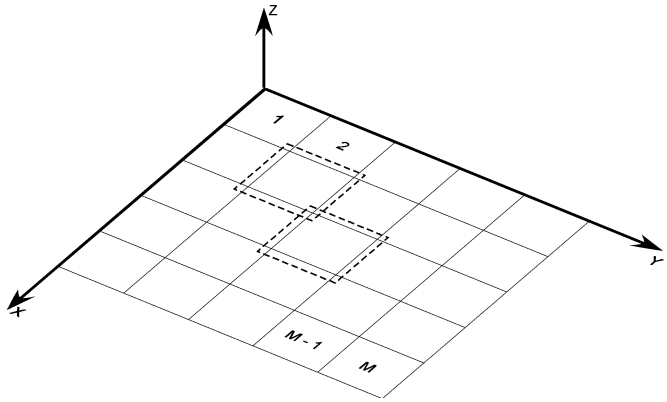

Fig. 3. Geometry of a PEC plate divided into 25 blocks. Extended blocks are represented in dashed lines.

a matrix $\mathbf{V}_{ii}^{\mathrm{PWS}}$, whose size is $N_{be} \times N_\phi N_\theta$. After exciting the block, $N_\phi N_\theta$ primary CBFs are determined for each block by solving the following linear system of equations:

$$\mathbf{Z}_{ii}^{\mathrm{ext}} \cdot \mathbf{J}_{ii}^{\mathrm{CBFs}} = \mathbf{V}_{ii}^{\mathrm{PWS}} \tag{2}$$

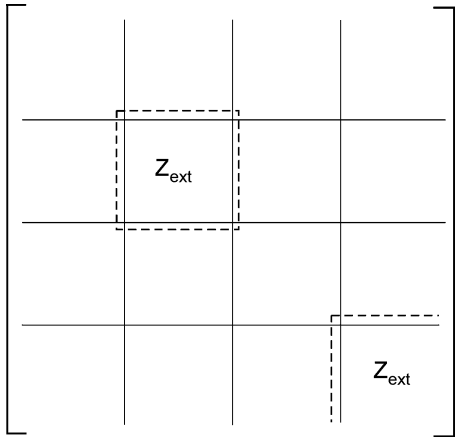

Fig. 4. MoM matrix segmentation procedure. Individual and extended blocks are shown in solid and dotted line, respectively.

where $\mathbf{J_{ii}}$ is an $N_{be} \times N_\phi N_\theta$ matrix, representing of the CBFs, as yet untruncated, for block i $(i = 1, 2, \ldots, M)$. Next, the above CBFs are truncated by discarding the current weight coefficients belonging to the extension region, so that the resulting CBFs are now confined within the original block, and their size is now reduced to $N_b \times N_\phi N_\theta$. Even though the size N of the complete MoM matrix may be very large because the original structure is large in terms of the wavelength, the dimension of each block can still be kept to a manageable level and, hence, the linear system (2) can be solved by using LU decomposition. This factorization is highly desirable since we have to solve (2) $N_\phi N_\theta$ times, one for each incident plane wave, to compute the complete set of primary basis functions.

Typically, the number of plane waves we have used to generate the CBFs would exceed the number of degrees of freedom (DoFs) associated with the block, and it is desirable to remove the redundancy in the basis functions by applying a singular value decomposition (SVD) procedure, and thresholding $\mathbf{J_{ii}}$. This is done by expressing this latter as

$$\mathbf{J}_{ii}^{\mathrm{CBFs}} = \mathbf{U}\mathbf{D}\mathbf{V}^t, \quad i = 1, 2, \ldots\ldots, M \tag{3}$$

where $\mathbf{U}$ is an $N_{be} \times N_\phi N_\theta$ orthogonal matrix, $\mathbf{V^t}$ is an $N_\phi N_\theta \times N_{be}$ orthogonal matrix, and $\mathbf{D}$ is an $N_\phi N_\theta \times N_\phi N_\theta$ diagonal

matrix. The elements of the diagonal matrix are the singular values of $\mathbf{J}_{ii}$. Next, we construct a new set of basis functions that are linear combinations of the original CBFs via the SVD approach, and only those with relative singular values above a certain threshold are retained. The threshold is chosen by normalizing the singular values with respect to the maximum. We then discard those normalized values (set them equal to zero) which fall below the threshold, typically chosen to be 10^{-3}, to set the level of accuracy we desire. This filtering process of eliminating the post-SVD CBFs is important to reduce their redundancy and, consequently, improve the condition number of the reduced matrix. For the sake of simplicity, we assume that all of the blocks contain the same number K of CBFs after SVD, where K is always smaller than $N_\phi N_\theta$.

It is worthwhile mentioning that the "new" primaries have all the desired characteristics of wavelets in terms of orthogonality and oscillatory behavior, though, in contrast to the wavelets, they are tailored to the geometry of the object. Thus, unlike the wavelets, the post-SVD CBFs can be used for an arbitrary three-dimensional object, without any restrictions.

Following the procedure described above, we construct KM primary basis functions, K for each of the M blocks. The solution to the entire problem is then expressed as a linear combination of the CBFs as follows:

$$\mathbf{J} = \sum_{k=1}^{K} \alpha_k^{(1)} \begin{bmatrix} \left[\mathbf{J}_k^{(1)}\right] \\ [0] \\ \vdots \\ [0] \end{bmatrix} + \sum_{k=1}^{K} \alpha_k^{(2)} \begin{bmatrix} [0] \\ \left[\mathbf{J}_k^{(2)}\right] \\ \vdots \\ [0] \end{bmatrix} + \cdots \cdots + \sum_{k=1}^{K} \alpha_k^{(M)} \begin{bmatrix} [0] \\ [0] \\ \vdots \\ \left[\mathbf{J}_k^{(M)}\right] \end{bmatrix} \quad (4)$$

where $\alpha_k^{(m)}$, for $m = 1, 2, \ldots, M$, are the unknown expansion coefficients to be determined by using the reduced matrix, and $\mathbf{J}_k^{(m)}$ is the k^{th} CBF of block m, for $k = 1, 2, \ldots K$. The final step is to generate the reduced $KM \times KM$ MoM matrix for the KM unknown complex coefficients α_k by performing the inner product on (1) once that $\mathbf{J}$ has been replaced by expression (4).

The reduced coefficient matrix has the form shown in (5), at the bottom of the page, where $\mathbf{Z}_{mn}$ is the coupling matrix linking the original (unextended) blocks m, and n, $\mathbf{Z}_{ii}$ is the dense self-coupling matrix of these blocks, $\mathbf{J}_{ii}$ is the truncated-CBFs matrix of block i after SVD. Note that each of the inner product entries in the above matrix results in a sub-matrix of size $K \times K$, and the MoM matrix reduction involves MK^2 complex matrix-vector products.

After performing the necessary operations indicated in (5), the original MoM matrix in (1) is reduced to a smaller one. The induced surface current distribution for the entire structure can now be obtained by substituting the values of α_k in (4). Once the current density distribution has been derived, the electrical parameters such as RCS, scattered field, etc., can be computed.

The most computationally intensive part of the proposed method is associated with the generation of the primary CBFs and the matrix reduction procedure. However, the latter task can be speeded up by observing that the following relationship holds:

$$\left\langle \mathbf{J}_{mm}^t \mathbf{Z}_{mn} \mathbf{J}_{nn} \right\rangle = \left\langle \mathbf{J}_{mm}^t \mathbf{Z}_{mn} \mathbf{J}_{nn} \right\rangle^t = \left\langle \mathbf{J}_{nn}^t \mathbf{Z}_{nm} \mathbf{J}_{mm} \right\rangle \quad (6)$$

since $\mathbf{Z}_{mn}^t = \mathbf{Z}_{nm}$. By using this observation, the complexity in computing (5) is reduced by a factor of two, since we can generate only the upper or lower triangular parts of the reduced matrix. Generation of CBFs is one of the time-consuming and memory-demanding task. It requires the filling the self-impedance matrix $\mathbf{Z}_{ii}$ for the extended block and its factorization in an LU form. Since the CBFs are independent of the incident angles, this factorization needs to be performed only once, and the resulting primaries can be reused for multiple incident angle directions. This implies that the final reduced matrix (5) is independent of the excitation, and this fact enables us to solve a problem involving multiple excitations by only solving the reduced system for the new $r.h.s.$ (excitation). Moreover, we can store the reduced matrix on the hard disk and reuse it whenever we need to analyze a new excitation. Furthermore, if the geometry within a particular block is modified, only the CBFs belonging to this block need to be recomputed.

The technique described above realizes a saving in the CPU running time and RAM requirement with respect to a conventional MoM technique. The memory requirement is now proportional to the square of the self impedance matrix of the extended block, and this is different from that in the conventional MoM where the storage requirement is related to the square of the dimension of the entire impedance matrix. Moreover, we realize a consistent saving in the execution time, which becomes $MO((N_{be})^3)$, as estimated by accounting for the largest computational burden. An order of the computational cost can be estimated by

$$\text{Cost} = \frac{M}{P} O\left(N_{be}^3\right) \quad (7)$$

where P is the number of processors. By choosing smaller blocks, we can further reduce the running time. An example is given in the numerical section, namely the corner reflector, for

$$[\mathbf{Z}]_{KM \times KM} = \begin{bmatrix} \langle \mathbf{J}_{11}^t \mathbf{Z}_{11} \mathbf{J}_{11} \rangle & \langle \mathbf{J}_{11}^t \mathbf{Z}_{12} \mathbf{J}_{22} \rangle & \cdots & \langle \mathbf{J}_{11}^t \mathbf{Z}_{1M} \mathbf{J}_{MM} \rangle \\ \langle \mathbf{J}_{22}^t \mathbf{Z}_{21} \mathbf{J}_{11} \rangle & \langle \mathbf{J}_{22}^t \mathbf{Z}_{22} \mathbf{J}_{22} \rangle & \cdots & \langle \mathbf{J}_{22}^t \mathbf{Z}_{2M} \mathbf{J}_{MM} \rangle \\ \vdots & \vdots & \ddots & \vdots \\ \langle \mathbf{J}_{MM}^t \mathbf{Z}_{M1} \mathbf{J}_{11} \rangle & \langle \mathbf{J}_{MM}^t \mathbf{Z}_{M2} \mathbf{J}_{22} \rangle & \cdots & \langle \mathbf{J}_{MM}^t \mathbf{Z}_{MM} \mathbf{J}_{MM} \rangle \end{bmatrix} \quad (5)$$

TABLE I
COMPARISON OF COMPUTATIONAL AND MEMORY PERFORMANCE FOR DENSE MATRIX AND SPARSE MATRIX APPROACHES

Problem Size	**Dense Matrix Approach**		**Sparse Matrix Approach, $d_0 = 0.15\lambda$**		
Unknowns	Filling Time (sec.)	RAM Requirement (Kb)	Filling Time (sec.)	RAM (Kb)	Sparsific-ation Rate (%)
1704	14.796	14297	3.187	545	97.5
3207	52.26	80350	10.828	2028	97.51
5979	179.53	279282	35.802	6624	97.628
9507	461.6	706117	101.593	25345	96.41

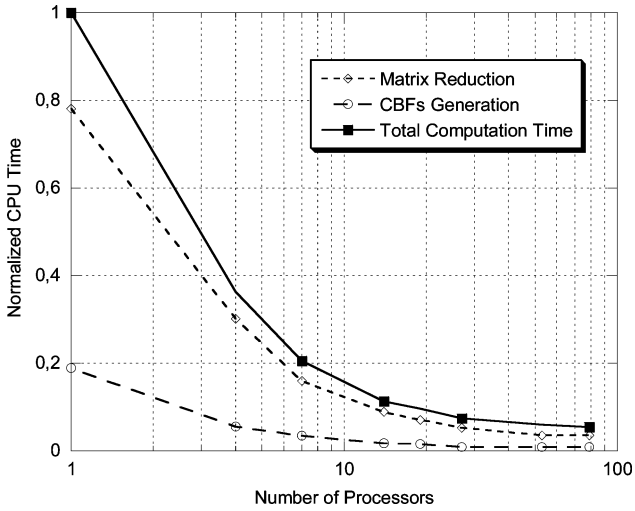

Fig. 5. Normalized CPU time of parallel CBMoM code.

which the geometry was first divided into 25, and then into 90 blocks.

It is worthwhile to point out that the CBFM is a highly parallelizable algorithm, because each block can be analyzed on a stand-alone basis on a parallel platform. Fig. 5 shows the time performance for the parallel CBF code based on MPI for a generic scattering problem ($N = 180.000$, $M = 40$, $N_{be} = 5.000$, for this example).

To further reduce the storage and time requirements of the proposed method, a new approach for generating primary CBFs is presented in the following section. It is based on the use of sparse representation of self-block impedance matrix.

III. SPARSE MATRIX APPROACH

We recall from the discussion in Section II, that the linear system (2) needs to be solved to compute a complete set of primary basis functions. Since, the coefficient matrix is complex and dense, this process may require large storage, and a long CPU time. In fact, the generation and inversion of the $\mathbf{Z_{ii}}$ matrix consume a considerable portion of the total solution time. The prime contributor to the matrix fill-time is the repeated numerical evaluation of the surface integrals over the testing and expansions functions involving the Green's function. Moreover, $\mathbf{Z_{ii}}$ may contain redundant information, resulting from the dense sampling rates of fields. To reduce the computational burden and the memory requirement in filling and solving the linear system (2), a sparse representation of the $\mathbf{Z_{ii}}$ matrix can be generated if we confine the computation of the field radiated by the individual sub-domain basis function only to its near neighborhood in the block. In particular, for each sub-domain basis function, the block surface is divided into two regions, viz., a near-field and a far-field region. The near-field region is spherical with a radius equal to d_0. Interactions within the near field are modelled in the customary MoM manner, leading to a dense set of entries near the diagonal of the matrix. In the far-field region, however, the sampling rate can be lower because the spectral content of the field is relatively low. The contributions of the far-field region can be neglected for the purpose of generating the CBFs though these interactions are included rigorously in the process of constructing the reduced matrix [see (5)]. It is important to recognize that the CBFs are not the final solution: they can be interpreted as merely macro-basis functions. This, in turn, enables us to generate these basis functions using sparsified matrix, without compromising the accuracy of the final solution. In particular, we have found that retaining the interaction within the distance of $d_0 = 0.15\lambda$ is sufficient to obtain a good representation of the CBFs for computing the final current distribution as well as the far field pattern accurately. As a consequence, we not only save time because the matrix generating the CBFs is sparse, but also memory because we do not need to store the matrix elements corresponding to the far-field interactions while generating the CBFs. This, in turn, enables us to enlarge the electrical size of each block and, consequently, the size of the reduced matrix. Moreover, we can solve the linear system (2) by using sparse matrix solvers. Table I compares the computational and memory costs of the proposed method against that needed to generate the CBFs in the conventional way (concerning the fill time, it is useful to point out that a "patch by patch" subroutine is used in the case of regular CBMoM approach, whereas an "edge by edge" procedure is employed for the sparse approach, being the former approach faster of a factor 9). It is evident that we can achieve a significant reduction both in the computational time and in the memory requirement by using the technique described above, without compromising the accuracy of the final solution, as we show in the next section. The same is not true, however, for the conventional MoM, where the loss of accuracy can be significant when we work with a sparse version of the Z matrix, and neglect the far-field interaction entirely.

IV. NUMERICAL RESULTS

The proposed technique has been applied to several different test examples to calculate the bi-static or mono-static RCS and the results have been compared with those derived by using a

direct or analytical computation to validate the method. The test cases chosen are: *i*) a 10λ side PEC cube; *ii*) a 4λ radius PEC sphere; *iii*) NASA almond; and *iv*) a corner reflector.

A. 10λ Side PEC Cube

To illustrate the accuracy and the efficiency of the proposed CBFM, we present the results for the problem of scattering by a PEC cube of 10λ side at a frequency of 300 MHz. The object is excited by a normally incident ($\theta = 0°$, $\phi = 0°$) theta-polarized plane wave. The discretization is carried out by using triangular patches with a mean edge length of 0.1λ, resulting in a problem with 180.000 unknowns. The geometry is divided into 56 blocks with an average size of 4.000 unknowns. Each block has been extended by $\Delta = 0.4\lambda$ in all directions and analyzed for a spectrum of plane waves incident from $0° \leq \theta < 180°$ and $0° \leq \phi < 360°$, with $N_\theta = N_\phi = 20$. This results in a total of 800 CBFs for each block, but, after SVD, only 200 (average value) are retained on each block. The 180.000×180.000 MoM matrix is then reduced to an 11.047×11.047 matrix and solved directly. The geometry has been analyzed by using both dense and sparse approaches. Moreover a comparison against a fast multiple method has been carried out. The sparse matrix approach allows us to reduce the computational cost of the analysis by a factor of approximately 3,35. In fact, the total time for CBFs generation is 2.699 s for regular approach and only 805 s for sparse approach. The total simulation time for the regular procedure has been 93.056 s, but the most of it is taken for the matrix reduction task. It is worthwhile to mention that we can solve bigger problems on a parallel architecture by using a parallel solver for the reduced matrix. In fact, the maximum size of the reduced-matrix, that can be stored into the RAM, is actually bounded by the maximum available memory on the solving process. The bi-static E-plane RCS, and the relative error are presented in Figs. 6 and 7, respectively, for dense approach, sparse approach, and FMM, and they show an excellent agreement at all scattering directions, including the grazing angles. It is important to point out that this type of large problem is not easily solvable with the conventional MoM codes without using iterations even on a Multi-CPU workstation, because of large memory requirement.

B. 4λ Radius PEC Sphere

In order to get a comparison with an analytical solution, we present the results for the problem of scattering by a PEC sphere of radius 4λ at a frequency of 300 MHz. The object is excited by a normally incident ($\theta = 0°$, $\phi = 0^{\phi}$) theta-polarized plane wave. The discretization is carried out by using triangular patches with a mean edge length of 0.1λ, resulting in a problem with 85.155 unknowns. The geometry is divided into 16 blocks with an average size of 8.000 unknowns. Each block has been extended by $\Delta = 0.4\lambda$ in all directions and analyzed for a spectrum of plane waves incident from $0° \leq \theta < 180°$ and $0° \leq \phi < 360°$, with $N_\theta = N_\phi = 20$. This results in a total of 800 CBFs but, after SVD, only 310 are retained on each block. The 85.155×85.155 MoM matrix is then reduced to a 4.925×4.925 matrix and solved directly. The geometry has been analyzed by using both dense and sparse approaches.

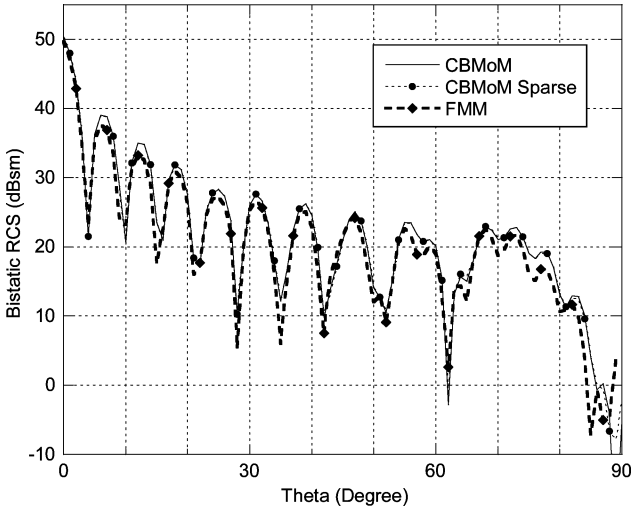

Fig. 6. Bistatic RCS of a 10λ metallic cube at 0.3 GHz, for horizontal polarization, computed by using regular CBMoM, sparse approach CBMoM, and FMM.

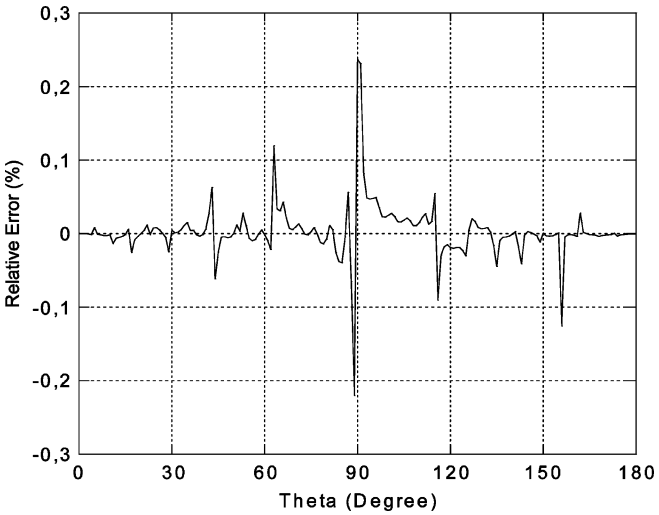

Fig. 7. Relative error (%) between the regular and sparse CBMoM approaches for the 10λ metallic cube at 0.3 GHz.

The sparse matrix approach allows us to reduce the computational cost of the analysis by a factor of approximately 3,8. The bi-static E- and H-plane RCS are presented in Fig. 8(a) and (b), respectively, for dense approach, sparse approach, and MIE series, and they show an excellent agreement at all scattering directions, including the grazing angles.

C. NASA Almond

Next, we choose a moderate size problem to demonstrate the accuracy and the efficiency of the proposed method in analyzing an electrically medium-size problem for a wide range of incident angles. In this case, we are interested in analyzing the mono-static RCS of a PEC NASA almond. In fact, the CBMoM shows all of its potentiality in this kind of analysis since, once the reduced matrix has been computed, all different excitations are calculated with a very small time compared to other approach. This target is shown in the insets of Figs. 9 and 10. Its total length is 25 cm along axis. The structure is divided into 2

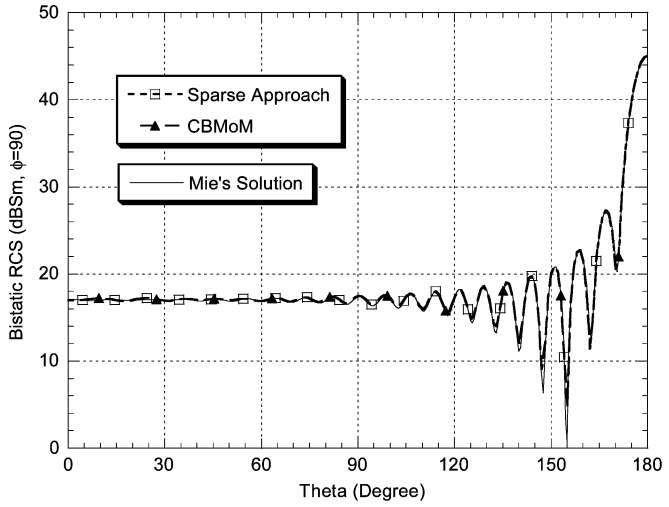

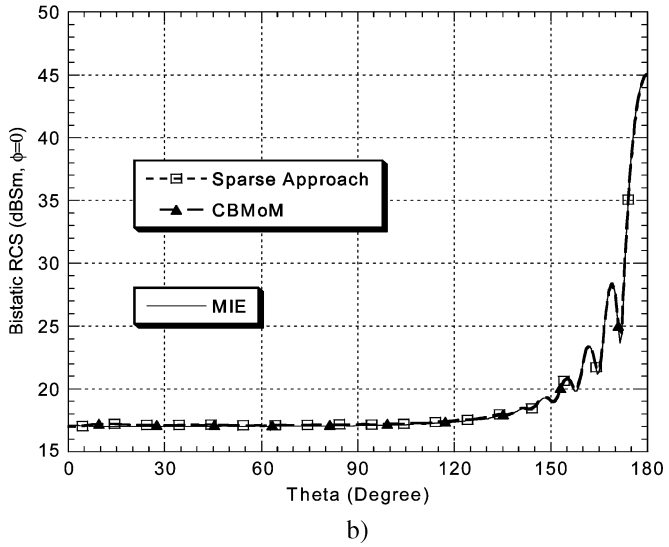

Fig. 8. Bistatic RCS of 4λ radius PEC sphere at 0.3 GHz: (a) E-plane; (b) H-plane.

blocks leading to a reduced matrix size of 500×500, derived by using the CBFM, and we observe that the size is considerably smaller than the original 14.736×14.736 matrix. In Figs. 9 and 10, the RCS for both the horizontal (HH) and vertical (VV) polarizations are plotted in dBSm (dB with respect to 1 square meter) as a function of the azimuthal angle. The elevation angle is zero, and the zero degree in azimuth corresponds to incidence along the tip. The RCS pattern is computed at a frequency of 7 GHz and compared against some measurements found in the open literature [15]. Although there are some discrepancies between the numerical results, obtained by using the sparse approach, and measurements, the overall agreement is seen to be good. One of the principal advantages of the proposed method lies in its ability to compute the mono-static RCS for multiple incident angles in a very efficient manner. In fact, once the reduced matrix has been computed, the solution takes only 4,5 s for each new incident angle, because the reduced matrix does not depend upon the excitation. The total simulation time, for the entire set of angles for this problem, is 8.100 s.

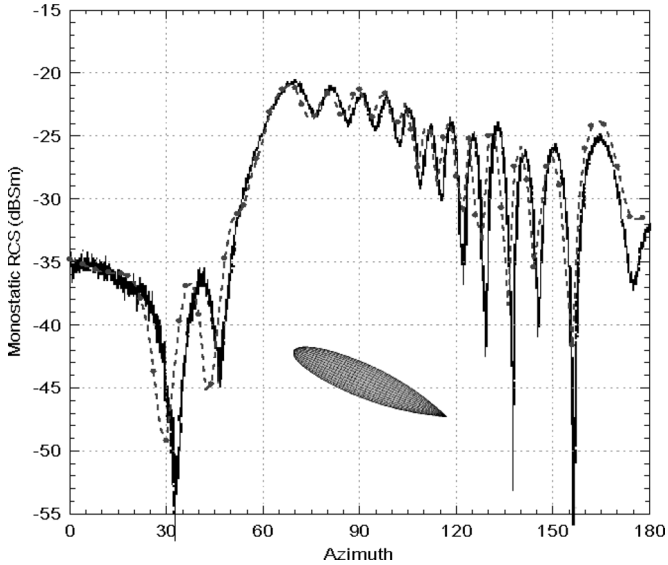

Fig. 9. Monostatic RCS of NASA metallic Almond at 7 GHz, for horizontal polarization, computed by using this method (dashed line with dots) and compared against measurements in [15] (continuous line).

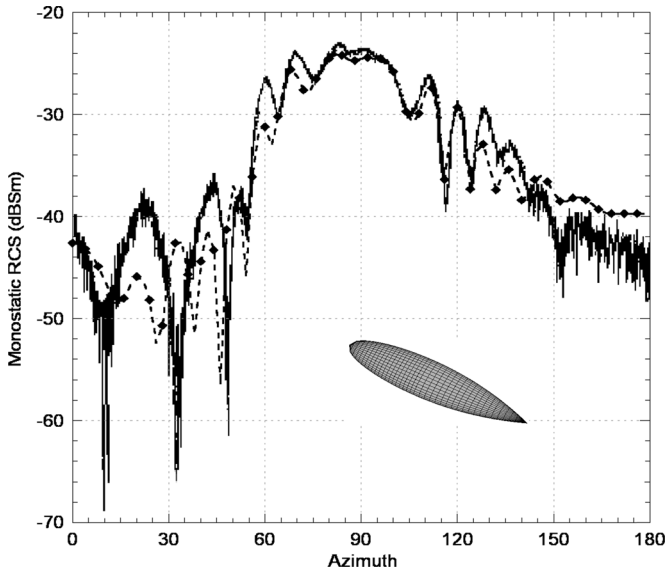

Fig. 10. NASA metallic almond at 7 GHz, for vertical polarization. The meaning of lines is the same as in the previous figure.

D. Corner Reflector

As a last example, we consider a corner reflector to further illustrate the application of the proposed methodology to objects that support multiple scattering. The geometry of the problem is represented in the inset of Fig. 11, and the dimensions of the rectangular plates composing the reflector are $20\lambda \times 10\lambda$. The entire structure has been divided into 25 blocks, each block is extended by $\Delta = 0.4\lambda$ in all directions, and excited by using multiple plane waves with $N_\theta = N_\phi = 20$ for a total of 800 pre-SVD CBFS. On average, only 220 singular values are retained in each block after the SVD. The original 119.600×119.600 MoM matrix is then reduced to a smaller one, whose size is 5.504. This geometry has been analyzed by using both sparse and dense matrix approaches, however, only the sparse

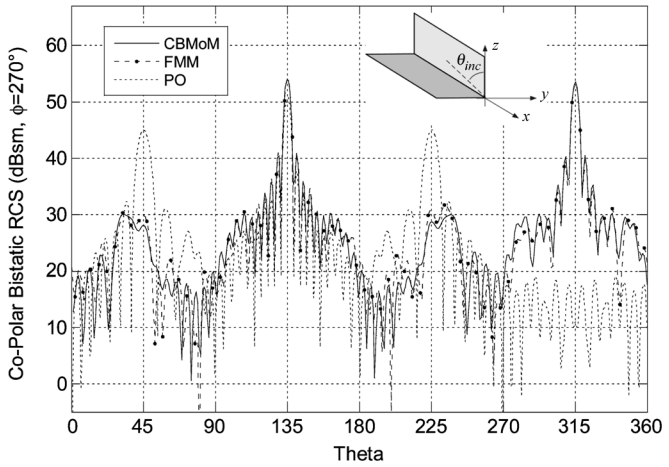

Fig. 11. Bistatic RCS (co-polar component) on the YZ plane for the metallic corner reflector, for a θ-polarized plane wave incident from ($\theta = 45°$, $\phi = 270°$), computed by using sparse CBMoM, FMM, and PO. The corner reflector geometry is shown in the inset and the dimensions of the rectangular plates forming the corner reflector are $20\lambda \times 10\lambda$.

results are plotted here to avoid overcrowding the plots. The results are compared to those obtained by using the FMM and PO. In particular, Fig. 11 depicts a theta-polarized plane wave incident from ($\theta = 45°$, $\phi = 270°$). The incident angle was deliberately chosen so that double reflections could occur. The result for the bistatic RCS for the co-polar component is compared with those from the FMM, as well as the PO. It is evident that our results agree well with FMM (also considering that our built-in MoM of CBMOM uses triangular patch and RWG basis functions, whereas FMM code employs rectangular patches and roof-top basis functions), while the PO does not perform well in the back-scattering region, and fails to predict the RCS levels correctly at $\theta = 45°$, and $\theta = 225°$. The cross-polarized component is not plotted here since it is 60 dB lower than the co-polar one, but we did find that the PO predictions are relatively poor for this component. The total time simulation is 96.070 s when 25 blocks are used. It is worthwhile to point out that the computational time can be further reduced by using smaller blocks. In particular, the run-time was found to reduce by a factor 1,95 when the geometry was divided into 90 blocks, without a loss of accuracy.

V. Conclusion

In this paper, an efficient technique to solve large and dense systems of linear equations arising in the electric field integral-equation formulation of an electromagnetic problem has been presented. Extension to the CFIE is currently under investigation and we foresee no difficulties in implementing it. The proposed method is based on splitting the original problem geometry analysis into several smaller sub-problems, by using a geometric division into so called blocks. We have demonstrated the effectiveness and accuracy of the proposed scheme via several numerical examples. We have also shown that the CBFM achieves a reduction in the CPU time and memory compared to the conventional MoM, and, mainly, it can solve electrically very large problems without the use of iterations. Dividing the original large structures into blocks provides two important advantages. First, if the geometry of the object is only altered locally within one of these blocks, the new CBFs need only be generated for that block. Second, in contrast to the conventional MoM, it renders the CBFM to be a naturally parallel algorithm, since it enables us to parcel off different blocks to different processors while generating CBFs. Finally, before closing we mention that the CBFM can be easily extended to radiation problems by adding the local source into the right hand side of (2) in the process of generating the CBFs. The details will appear in a further publication.

References

[1] S. M. Rao, D. R. Wilton, and A. W. Glisson, "Electromagnetic scattering by surfaces of arbitrary shape," *IEEE Trans. Antennas Propag.*, vol. AP-30, pp. 409–412, May 1982.

[2] R. G. Kouyoumjian, "The geometrical theory of diffraction and its application," in *Numerical and Asymptotic Techniques in Elettromagnetics*, R. Mittra, Ed. Berlin, Heidelberg, New York: Springer-Verlag, 1975.

[3] P. Y. Ufimtsev, "Elementary edge waves and the physical theory of diffraction," *Electromagn.*, vol. 11, no. 2, pp. 125–159, Apr./Jun. 1991.

[4] G. A. Thiele and G. A. Newhouse, "A hybrid technique for combining moment methods with the geometrical theory of diffraction," *IEEE Trans. Antennas Propag.*, vol. AP-23, pp. 551–558, Jul. 1975.

[5] F. X. Canning, "Solution of IML form of moment method problems in 5 iterations," *Radio Sci.*, vol. 30, no. 5, pp. 1371–1384, Sep./Oct. 1995.

[6] R. L. Wagner and W. C. Chew, "A study of wavelets for the solution of electromagnetic integral equations," *IEEE Trans. Antennas Propag.*, vol. 43, pp. 802–810, Aug. 1995.

[7] A. Boag and R. Mittra, "Complex multipole beam approach to electromagnetic scattering problems," *IEEE Trans. Antennas Propag.*, vol. 42, pp. 366–372, Mar. 1994.

[8] E. Michielssen and A. Boag, "Multilevel evaluation of electromagnetic fields for the rapid solution of scattering problems," *Microw. Opt. Technol. Lett.*, vol. 7, pp. 790–795, Dec. 5, 1994.

[9] R. Coifman, V. Roklin, and S. Wandzura, "The fast multipole method for the wave equation: A pedestrian prescription," *IEEE Antennas Propag. Mag.*, vol. 35, pp. 7–12, Jun. 1993.

[10] J. Song, C. Lu, and W. C. Chew, "Multilevel fast multipole algorithm for electromagnetic scattering by large complex objects," *IEEE Trans. Antennas Propag.*, vol. AP-45, pp. 1488–1493, Oct. 1997.

[11] E. Suter and J. Mosig, "A subdomain multilevel approach for the MoM analysis of large antennas," *Microw. Opt. Techno. Lett.*, vol. 26, pp. 270–277, 2000.

[12] V. V. S. Prakash and R. Mittra, "Characteristic basis function method: A new technique for efficient solution of method of moments matrix equation," *Microw. Opt. Techno. Lett.*, vol. 36, no. 2, pp. 95–100, Jan. 20, 2003.

[13] H. Haddar, S. Kusiak, and J. Sylvester, "The convex backscattering support," *SIAM J. Math. Anal.*, vol. 66, pp. 591–615, 2005.

[14] O. Bucci and G. Franceschetti, "On the spatial bandwidth of scattered fields," *IEEE Trans. Antennas Propag.*, vol. AP-35, pp. 1445–1455, Oct. 1997.

[15] A. C. Woo, H. T. G. Wang, M. J. Schuh, and M. L. Sanders, "Benchmark radar targets for the validation of computational electromagnetic programs," *IEEE Antennas Propag. Mag.*, vol. 35, no. 1, pp. 84–89, Feb. 1993.

Eugenio Lucente received the "Laurea" degree in telecommunication engineering from the University of Pisa, Pisa, Italy, in 2003.

In 2003–2004, he was a Visiting Student at the Electromagnetic Communication Laboratory, Pennsylvania State University (Penn State), University Park. In October 2004, he joined the Microwave and Radiation Laboratory, Department of Information Engineering, University of Pisa, where he is currently enrolled in the Ph.D. program. He has been collaborating with the Electromagnetic Communication Laboratory, Penn State University, since 2004. His research interests include frequency- and time-domain numerical methods for solving electrically large electromagnetic problems.

Agostino Monorchio (S'89–M'96–SM'04) was born in Italy on March 16, 1966. He received the Laurea degree in electronics engineering and the Ph.D. degree in methods and technologies for environmental monitoring from the University of Pisa, Pisa, Italy, in 1991 and 1994, respectively.

During 1995, he joined the Radio Astronomy Group, Arcetri Astrophysical Observatory, Florence, Italy, as a Postdoctoral Research Fellow, working in the area of antennas and microwave systems. He has been collaborating with the Electromagnetic Communication Laboratory, Pennsylvania State University (Penn State), University Park, where he is an Affiliate of the Computational Electromagnetics and Antennas Research Laboratory. He has been a Visiting Scientist at the University of Granada, Spain, and at the Communication University of China in Beijing. He is currently an Associate Professor in the School of Engineering, University of Pisa, and Adjunct Professor at the Italian Naval Academy of Livorno. He is also an Adjunct Professor in the Department of Electrical Engineering, Penn State. He is on the Teaching Board of the Ph.D. course in "Remote Sensing" and on the council of the Ph.D. School of Engineering "Leonardo da Vinci" at the University of Pisa. His research interests include the development of novel numerical and asymptotic methods in applied electromagnetics, both in frequency and time domains, with applications to the design of antennas, microwave systems and RCS calculation, the analysis and design of frequency-selective surfaces and novel materials, and the definition of electromagnetic scattering models from complex objects and random surfaces for remote sensing applications. He has been a reviewer for many scientific journals. He has been supervising various research projects related to applied electromagnetics commissioned and supported by national companies and public institutions.

Dr. Monorchio is currently an Associate Editor of the IEEE ANTENNAS AND WIRELESS PROPAGATION LETTERS. He received a Summa Foundation Fellowship and a NATO Senior Fellowship.

Raj Mittra (S'54–M'57–SM'69–F'71–LF'96) is a Professor in the Electrical Engineering Department, Pennsylvania State University (Penn State), University Park. He is also the Director of the Electromagnetic Communication Laboratory, which is affiliated with the Communication and Space Sciences Laboratory of the Electrical Engineering Department. Prior to joining Penn State he was a Professor in Electrical and Computer Engineering Department, University of Illinois at Urbana Champaign. He has also been a Visiting Professor at Oxford University, Oxford, England and at the Technical University of Denmark, Lyngby, Denmark. His professional interests include the areas of Communication Antenna Design, RF circuits, computational electromagnetics, electromagnetic modeling and simulation of electronic packages, EMC analysis, radar scattering, frequency selective surfaces, microwave and millimeter wave integrated circuits, and satellite antennas. He has published over 900 journal and symposium papers and more than 40 books or book chapters on various topics related to electromagnetics, antennas, microwaves and electronic packaging. He also has three patents on communication antennas to his credit. He has supervised 90 Ph.D. theses, 90 M.S. theses, and has mentored more than 50 postdocs and visiting scholars. He has directed, as well as lectured in, numerous short courses on computational electromagnetics, electronic packaging, wireless antennas and metamaterials, both nationally and internationally.

Dr. Mittra is a Life Fellow of the IEEE, a Past-President of AP-S, and has served as Editor of the IEEE TRANSACTIONS ON ANTENNAS AND PROPAGATION.. He won the Guggenheim Fellowship Award in 1965, the IEEE Centennial Medal in 1984, the IEEE Millennium medal in 2000, the IEEE/AP-S Distinguished Achievement Award in 2002, the AP-S Chen-To Tai Distinguished Educator Award in 2004 and the IEEE Electromagnetics Award in 2006. He has also served as the North American Editor of the journal *AEÜ*